Space–time adaptive reduced-rank processor for interference mitigation in DS-CDMA systems

R.C. de Lamare and R. Sampaio-Neto

Abstract: A space–time adaptive reduced-rank processor for interference mitigation in DS-CDMA systems is proposed based on interpolated finite impulse response filters with time-varying interpolators. The proposed space–time processor allows a significant reduction in the number of estimation elements, thereby increasing the convergence and tracking performance of the estimation algorithms. In order to compute the parameters of the proposed space–time processor, a least squares design is presented and computationally efficient recursive least-squares (RLS) algorithms are developed for estimating the parameters of both reduced-rank receiver and interpolator. A linear and successive interference cancellation space–time receivers based on the proposed reduced-rank processor for mitigating multi-access and intersymbol interference in an uplink scenario are proposed. An analysis of the convergence properties of the proposed space–time processor is carried out and analytical expressions are derived for predicting the mean squared error performance of the proposed RLS algorithm. Simulation results show that the proposed reduced-rank space–time processor and RLS algorithms outperform existing techniques at lower complexity.

1 Introduction

In DS-CDMA systems, the incorporation of multiuser receivers in conjunction with antenna arrays can provide an enhanced performance for multi-access interference (MAI) and intersymbol interference (ISI) mitigation [1–3]. This requires the joint processing of the data received at an antenna array with elements closely spaced, which leads to the combination of multiuser detection and beamforming [4]. Multiuser detection exploits the temporal structure, whereas beamforming exploits the spatial structure of the interference. The literature presents several sub-optimal multiuser detectors capable of providing cost-effective interference mitigation: the linear [5] and decision feedback [6] receivers, the successive interference canceller (SIC) [7] and the parallel interference canceller (PIC) [8]. Among these detection strategies, interference cancellation (IC) techniques such as SIC and PIC are relatively simple and well suited for the uplink of DS-CDMA systems. At each stage, the PIC simultaneously regenerates and cancels from each user the MAI due to other users based on the detected symbols in the preceding stage. The SIC sequentially removes the MAI originated from the stronger users before detecting the weaker ones and presents some performance advantages over PIC and linear detectors [9, 10]. However, the design of these detectors with antenna arrays for combined multiuser detection and beamforming presents a major challenge due to the increased number of parameters to be estimated.

doi:10.1049/iet-com:20070265

Paper first received 19th July 2006 and in revised form 25th April 2007

R.C. de Lamare was with CETUC/PUC-RIO and is now with Communications Research Group, Department of Electronics, University of York, York Y010 5DD, U K.

R. Sampaio-Neto is with CETUC/PUC-RIO, Rio de Janeiro 22453-900, Brazil

E-mail: redl500@york.ac.uk

In order to estimate the parameters of space–time receivers in dynamic environments, the designer may resort to adaptive estimation algorithms that can track the highly dynamic conditions of the channels and usually have a good trade-off between performance and computational complexity. However, when the number of elements for estimation in the receiver is large, the task becomes rather challenging and one has to cope with an increased complexity and poor convergence performance. This is because the convergence speed of adaptive estimators are governed by the number of adaptive elements used in the estimation process. Reduced-rank interference suppression for DS-CDMA [11–18] is motivated by situations where the number of elements in the receiver is large and it is desirable to work with fewer parameters for complexity and convergence reasons. Several reduced-rank methods have been reported in the last decade, namely, the subspace detectors [11–13], the multistage Wiener filter (MWF) of Goldstein *et al.* in [14] and the recent adaptive finite impulse response (FIR) filters with adaptive interpolators [18]. The major problem with the MWF and eigen-decomposition techniques is that they rely on the full-rank covariance matrix $\boldsymbol{R}$ as a starting point for the subspace decomposition. The estimation process of a full-rank $\boldsymbol{R}$ with time averages can be problematic and experience tracking problems in dynamic situations.

In this work, we propose a reduced-rank space–time processor based on the recently reported joint adaptive interpolator and reduced-rank scheme [18] and derive a computationally efficient recursive least-squares (RLS) algorithm for parameter estimation. In contrast to the MWF, the proposed processor uses a projection based on interpolation and decimation operations and skips the processing stage with $\boldsymbol{R}$. The proposed scheme directly estimates (after the decimation) through time averages a reduced-rank covariance matrix, leading to convergence and tracking performance advantages over the MWF. An analysis of the global convergence properties of the proposed joint adaptive interpolator and reduced-rank estimation scheme, which is not treated in [18], is carried out and an evaluation of the computational complexity of the proposed space–time processor is presented. An analysis of the convergence properties of the proposed space–time processor is also conducted and analytical expressions are devised for predicting the mean squared error (MSE) performance of the proposed reduced-rank RLS algorithm. The second contribution of this paper is the proposal of linear and SIC antenna-array receivers designed with the proposed space–time processor and a comparative analysis of these receiver structures with schemes based on the full-rank [3] and the MWF [14–16] approaches.

This work is organised as follows. Section 2 describes an asynchronous space–time DS-CDMA system model. Section 3 presents the proposed space–time reduced-rank processor. The proposed space–time reduced-rank linear and SIC multiuser receivers are presented in Section 4, whereas Section 5 is devoted to the least-squares (LS) design of the parameter estimators. An RLS algorithm for the proposed processor is presented in Section 6 along with a convergence analysis of the reduced-rank algorithm and an evaluation of its computational complexity. Section 7 presents and discusses the simulation results, whereas Section 8 gives the conclusions.

2 DS-CDMA system model

Consider the uplink of an asynchronous binary phase shift keying DS-CDMA system with K users, N binary chips per symbol and L_p paths. The transmitted signal for the kth user is

$$x_k(t) = A_k \sum_{i=-\infty}^{\infty} b_k(i) s_k(t - iT) \tag{1}$$

where $b_k(i) \in \{\pm 1\}$ is the ith symbol for user k, the real-valued spreading waveform and the amplitude associated with user k are $s_k(t)$ and A_k, respectively. The spreading waveforms are given by $s_k(t) = \sum_{i=1}^{N} (a_k)(i)\phi(t - iT_c)$, where $a_k(i) \in \{\pm 1/\sqrt{N}\}$, $\phi(t)$ is the chip waveform, T_c is the chip duration and $N = T/T_c$ is the processing gain. Assuming that the receiver equipped with linear antenna arrays is synchronised with the main path and identical amplitude fading is experienced by all antenna elements for each path of each user signal (no antenna diversity), the coherently demodulated composite received signal at the lth antenna element is

$$r_l(t) = \sum_{k=1}^{K} \sum_{m=0}^{L_p - 1} h_{k,m}(t) e^{j\Theta_{k,m}} x_k(t - \tau_{k,m} - d_k) + n(t) \tag{2}$$

where $\theta_{k,m} = 2\pi(l-1)(d/\lambda)\cos(\phi_{k,m})$ the delay shift of the mth path of the kth user, $\phi_{k,m}$ is the direction of arrival (DoA) of the signal of user k and its mth path, $d = \lambda/2$ is the spacing between sensors and λ the carrier wavelength. The channel coefficient associated with the mth path and the kth user is $h_{k,m}(t)$, $d_k \in \{0, 1, \ldots, N-1\}$ is the asynchronism of the kth user and $\tau_{k,m}$ is the delay of the mth path of the kth user, which is assumed to be a multiple of the chip rate. We assume that the channel is constant during each symbol interval, the spreading codes are repeated from symbol to symbol, and the receiver with a J-element linear antenna array is synchronised with the main path. The complex envelope of the received waveforms after filtering by a chip-pulse matched filter and sampled at chip rate is collected and organised in a $JM \times 1$ observation vector corresponding to the ith signalling interval

$$\boldsymbol{r}(i) = \sum_{k=1}^{K} A_k b_k(i-1) \bar{\mathcal{F}} \mathcal{H}_k(i-1) + A_k b_k(i) \mathcal{F} \mathcal{H}_k(i)$$

where $M = N + L_p - 1$, the complex Gaussian noise vector is $\boldsymbol{n}(i) = [n_1(i) \ \ldots \ n_{JM}(i)]^T$ with $E[\boldsymbol{n}(i)\boldsymbol{n}^H(i)] = \sigma^2 \boldsymbol{I}$, $(\cdot)^T$ and $(\cdot)^H$ denote transpose and Hermitian transpose, respectively, and $E[\cdot]$ stands for expected value. The space–time convolution matrices $\mathcal{F}_k$ and $\bar{\mathcal{F}}_k$ have dimension $JM \times JL_p$ and contain matrices with special structures on their main diagonal, that is

$$\begin{aligned} \mathcal{F}_k &= \text{diag}(\mathcal{C}_k, \mathcal{C}_k, \ldots, \mathcal{C}_k) \quad \text{and} \\ \bar{\mathcal{F}}_k &= \text{diag}(\mathcal{C}_k, \bar{\mathcal{C}}_k, \ldots, \bar{\mathcal{C}}_k) \end{aligned} \tag{4}$$

The columns of the $M \times L_p$ matrix $\mathcal{C}_k$ contain one-chip shifted versions of segments of the signature sequence $\boldsymbol{s}_k = [a_k(1) \cdots a_k(N)]^T$ of user k given by

$$\begin{aligned} \boldsymbol{s}_k^{d_k} &= [c_k(1) \cdots c_k(N)]^T \\ &= [\underbrace{0 \cdots 0}_{d_k} \underbrace{a_k(1) \cdots a_k(N - d_k + 1)}_{N - d_k}]^T \end{aligned} \tag{5}$$

where d_k is the shift in chips that describes the system asynchronism. The structure of the $M \times L_p$ matrix $\mathcal{C}_k$ is described by

$$\mathcal{C}_k = \begin{bmatrix} c_k(1) & & \boldsymbol{0} \\ \vdots & \ddots & c_k(1) \\ c_k(N) & & \vdots \\ \boldsymbol{0} & \ddots & c_k(N) \end{bmatrix} \tag{6}$$

The structure of $\bar{\mathcal{C}}_k$ is analogous to $\mathcal{C}_k$ but employs the segments of $\boldsymbol{s}_k$ given by

$$\bar{\boldsymbol{s}}_k^{d_k} = [\underbrace{a_k(N - d_k + 1) \cdots a_k(N)}_{d_k} \underbrace{0 \cdots 0}_{N - d_k}] \tag{7}$$

The corresponding spatial signatures are

$$\begin{aligned} \bar{\boldsymbol{p}}_k^{d_k}(i-1) &= \bar{\mathcal{F}}_k \mathcal{H}_k(i-1) \quad \text{and} \\ \boldsymbol{p}_k^{d_k}(i-1) &= \mathcal{F}_k \mathcal{H}_k(i-1) \end{aligned} \tag{8}$$

The $JL_p \times 1$ space–time channel vector is given by

$$\mathcal{H}_k(i) = [\boldsymbol{h}_{k,0}^T(i) | \boldsymbol{h}_{k,1}^T(i) | \cdots | \boldsymbol{h}_{k,J-1}^T(i)]^T \tag{9}$$

where $\boldsymbol{h}_{k,l}(i) = [h_{k,0}^{(l)}(i) \cdots h_{k,\ L_{p-1}}(i)]^T$ is the $L_p \times 1$ vector with the channel gains of user k at sensor l. The spatial channels assume that the amplitudes do not vary across antenna elements; however, the directions of arrival are different for each user and path and the signals experience a phase shift [4, 14].

3 Proposed space–time reduced-rank processor

The principles of the proposed space–time adaptive reduced-rank (STAR) processor structure are detailed here. Fig. 1 shows the STAR processor, where an interpolator and a reduced-rank receiver that are time varying are employed. The received vector $\boldsymbol{r}(i) = [r_0^{(i)} \ \cdots \ r_{JM-1}^{(i)}]^T$ is filtered by the interpolator filter $\boldsymbol{v}_k(i) = [v_{k,0}^{(i)} \ \ldots \ v_{k,N_I-1}^{(i)}]^T$, yielding the interpolated received vector $\boldsymbol{r}_k(i)$ with JM samples. The $JM \times 1$ vector $\boldsymbol{r}_k(i)$ is then projected

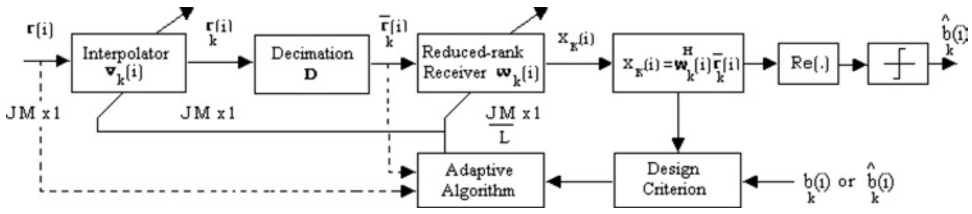

Fig. 1 *Proposed STAR processor*

onto a $JM/L \times 1$-dimensional vector $\bar{\boldsymbol{r}}_k(i)$. This corresponds to removing $L-1$ samples of $\boldsymbol{r}_k(i)$ of each set of L consecutive ones. Then the inner product of $\bar{\boldsymbol{r}}_k(i)$ with the parameter vector $\boldsymbol{w}_k(i) = [w_{k,0}^{(i)} \ \cdots \ w_{k,JM/L-1}]^{\mathrm{T}}$ is computed to obtain the estimate $x_k(i)$ before the slicer yields the detected symbol $\hat{b}_k(i)$, as depicted in Fig. 1.

The vector $\bar{\boldsymbol{r}}_k(i) = \boldsymbol{D}\boldsymbol{r}_k(i)$ is obtained with the aid of the $JM/L \times M$ projection matrix $\boldsymbol{D}$ that is mathematically equivalent to uniform decimation on $\boldsymbol{r}_k(i)$. The STAR processor with decimation factor L can be designed by choosing $\boldsymbol{D}$ as

$$\boldsymbol{D} = \begin{bmatrix} 1 & 0 & 0 & 0 & 0 & \dots & 0 & 0 & 0 & 0 & 0 \\ \vdots & \vdots & \vdots & \vdots & \vdots & \vdots & \vdots & \vdots & \vdots & \vdots & \vdots \\ \underbrace{0 \ \dots \ 0}_{(m-1)L \text{ zeros}} & & & 1 & 0 & \dots & 0 & 0 & 0 & 0 & 0 \\ \vdots & \vdots & \vdots & \vdots & \vdots & \ddots & \vdots & \vdots & \vdots & \vdots & \vdots \\ \underbrace{0 \ 0 \ 0 \ 0 \ 0 \ \dots \ 0}_{(JM/L-1)L \text{ zeros}} & & & & & & & 1 & \underbrace{0 \ \dots \ 0}_{(L-1) \text{ zeros}} & & \end{bmatrix} \tag{10}$$

where $m = 1, \dots, JM/L$ is the mth row. The strategy to design the interpolator and the receiver is to express the symbol estimate $x_k(i) = \boldsymbol{w}_k(i)\bar{\boldsymbol{r}}_k(i)$ as a function of $\boldsymbol{w}_k(i)$ and $\boldsymbol{v}_k(i)$

$$\begin{aligned} x_k(i) &= w_0^* \boldsymbol{v}_k^H \dot{\boldsymbol{r}}_0 + w_1^* \boldsymbol{v}_k^H \dot{\boldsymbol{r}}_1 + \cdots + w_{JM/L-1}^* \boldsymbol{v}_k^H \dot{\boldsymbol{r}}_{JM/L-1} \\ x_k(i) &= \boldsymbol{v}_k^H(i)[\dot{\boldsymbol{r}}_0^{(i)}| \cdots |\dot{\boldsymbol{r}}_{JM/L-1}^{(i)}]\boldsymbol{w}_k^*(i) \\ &= \boldsymbol{v}_k^H(i)\Re(i)\boldsymbol{w}_k^*(i) = \boldsymbol{v}_k^H(i)\boldsymbol{u}_k(i) \end{aligned} \tag{11}$$

where $\boldsymbol{u}_k(i) = \Re(i)\boldsymbol{w}_k{}^*(i)$ is a $N_I \times 1$ vector, $(\cdot)^*$ denotes complex conjugate, the JM/L coefficients of $\boldsymbol{w}_k(i)$ and the N_I elements of $\boldsymbol{v}_k(i)$ are complex and $\dot{\boldsymbol{r}}_s(i)$ is a length N_I segment of the received vector $\boldsymbol{r}(i)$ beginning at $r_{s \times L}(i)$ and

$$\Re(i) = \begin{bmatrix} r_0^{(i)} & r_L^{(i)} & \cdots & r_{(JM/L-1)L}^{(i)} \\ \vdots & \vdots & \ddots & \vdots \\ r_{N_I-1}^{(i)} & r_{L+N_I-1}^{(i)} & \cdots & r_{(JM/L-1)L+N_I-1}^{(i)} \end{bmatrix} \tag{12}$$

4 Space–time reduced-rank receivers

The combination of multiuser detection and beamforming can provide an enhanced performance for MAI and ISI suppression [1–3]. This requires the joint processing of the data received at an antenna array with elements closely spaced, leading to an increase in the number of parameters to be estimated. The problem of dealing with a high number of estimation elements will be addressed with the STAR processor. The aim of this section is to detail the proposed space–time linear and SIC receivers that are designed with the proposed STAR processor.

4.1 Space–time linear receivers

The STAR linear receiver design employs a FIR filter $\boldsymbol{w}_k(i)$ with JM/L elements to yield an estimate of the desired symbol

$$\hat{b}_k(i) = \mathrm{sgn}(\mathrm{Re}[\boldsymbol{w}_k^H(i)\bar{\boldsymbol{r}}_k(i)]) \tag{13}$$

where $\mathrm{Re}(\cdot)$ selects the real part, $\mathrm{sgn}(\cdot)$ the signum function and $\bar{\boldsymbol{r}}_k(i)$ the JM/L reduced-rank received vector provided by the STAR processor.

4.2 Space–time SIC receivers

In this section, we present a space–time SIC receiver based on the proposed STAR processor. The goal of this structure is to exploit IC to further enhance the capacity of the STAR processor as compared with a linear detector. The STAR–SIC receiver detects users in a multistage fashion using a STAR linear receiver front end. To this end, the proposed SIC scheme requires the ordering of the users and the estimation of their channels and amplitudes. The detector employs a bank of space–time RAKE receivers to provide the receiver with estimates of the power of the users, as shown in Fig. 2. At each symbol, the SIC algorithm [9, 10] selects users according to their power (decreasing power order) and then sequentially regenerates and cancels the interference contribution of every user at each stage. The detected symbols are described by

$$\hat{b}_k(i) = \mathrm{sgn}(\mathrm{Re}[\boldsymbol{w}_k^H(i)\bar{y}_k(i)]) \tag{14}$$

where the $JM/L \times 1$ vector $\bar{\boldsymbol{y}}_1(i) = \boldsymbol{D}(\boldsymbol{V}_1(i)\boldsymbol{r}(i)) = \bar{\boldsymbol{r}}_1(i)$ corresponds to user $k = 1$. Note that in this context, the first user denotes the one with the highest power level and does not benefit from IC. The $JM \times JM$ matrix $\boldsymbol{V}_k(i)$ is a convolution matrix with one-chip shifted versions of the $N_I \times 1$ interpolator $\boldsymbol{v}_k(i)$ of user k, the $JM/L \times 1$ reduced-rank received vector at each SIC stage is given by

$$\bar{\boldsymbol{y}}_k(i) = \boldsymbol{D}(\boldsymbol{V}_k(i)\boldsymbol{y}^{(k)}(i)), \quad k = 2, \dots, K \tag{15}$$

where

$$\begin{aligned} \boldsymbol{y}^{(k)}(i) = \boldsymbol{r}(i) - \Bigg(&\sum_{m=1}^{k-1} \hat{A}_m(i-1)\hat{b}_m(i-1)\hat{\bar{\boldsymbol{p}}}_m^{d_m}(i-1) \\ &+ \hat{A}_m(i)\hat{b}_m(i)\hat{\boldsymbol{p}}_m^{d_m}(i)\Bigg) \end{aligned} \tag{16}$$

is the $JM \times 1$ received signal at the kth stage, $\hat{A}_m$ the mth user amplitude estimate and the $JM \times 1$ spatial signature estimates are $\hat{\bar{\boldsymbol{p}}}_m^{d_m}(i-1) = \bar{\mathcal{F}}_k\hat{\mathcal{H}}_j(i)$ and $\hat{\boldsymbol{p}}_m^{d_m}(i) = \mathcal{F}_k\hat{\mathcal{H}}_k(i)$. In order to compute the spatial signature estimates and carry out IC, the designer has to estimate the channels and amplitudes of the users. This important task is considered in the next sections.

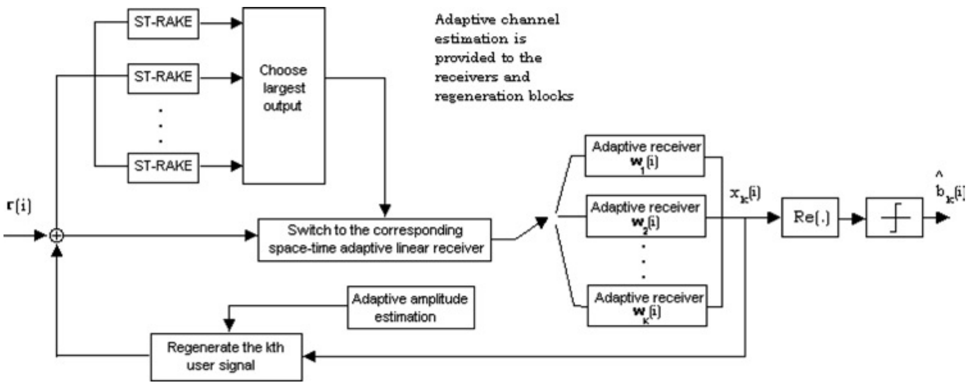

Fig. 2 *Proposed space-time adaptive SIC receiver*

4.2.1 Space–time channel estimation: Unlike the single-antenna existing approaches [19], the space–time channel estimation for the SIC receiver exploits the IC, resulting in enhanced channel estimates for users that benefit from the SIC scheme. In order to describe the channel estimator, we define the matrix $\tilde{\mathcal{C}}_k$ with one-chip shifted versions of the signature sequence for user k and the block diagonal matrix $\tilde{\mathcal{F}}_k$ given by

$$\tilde{\mathcal{C}}_k = \begin{bmatrix} a_k(1) & & \mathbf{0} \\ \vdots & \ddots & a_k(1) \\ a_k(N) & \ddots & \vdots \\ \mathbf{0} & \ddots & a_k(N) \end{bmatrix}, \qquad (17)$$

$$\tilde{\mathcal{F}} = \begin{bmatrix} \tilde{\mathcal{C}}_k & \dots & \mathbf{0} \\ \vdots & \ddots & \vdots \\ \mathbf{0} & \dots & \tilde{\mathcal{C}}_k \end{bmatrix}$$

Note that the above matrix $\tilde{\mathcal{C}}_k$ has a structure similar to the one of $\bar{\mathcal{C}}_k$ and equals $\boldsymbol{\mathcal{C}}_k$ defined in (4) for $d_k = 0$. Let us also define an $2M \times 1$-dimensional vector that corresponds to the received data for two consecutive symbol intervals at sensor j

$$\boldsymbol{r}_j^c(i) = \begin{bmatrix} \boldsymbol{r}(i) \\ \boldsymbol{r}(i+1) \end{bmatrix}$$

$$= \sum_{k=1}^{K} A_k(i-1)b_k(i-1)\begin{bmatrix} \bar{\mathcal{C}}_k \\ \mathbf{0}_M \end{bmatrix}\boldsymbol{h}_{k,j}(i-1)$$

$$+ A_k(i)b_k(i)\begin{bmatrix} \mathbf{0}_{d_k} \\ \tilde{\mathcal{C}}_k \\ \mathbf{0}_{M-d_k} \end{bmatrix}\boldsymbol{h}_{k,j}(i)$$

$$+ A_k(i+1)b_k(i+1)\begin{bmatrix} \mathbf{0}_M \\ \mathcal{C}_k \end{bmatrix}\boldsymbol{h}_{k,j}(i+1) + \boldsymbol{n}^c(i) \qquad (18)$$

In order to estimate the channel $\boldsymbol{h}_{k,j}(i)$ at each sensor, we consider the following optimization

$$\hat{\boldsymbol{h}}_{k,j}(i) = \arg\min_{\hat{\boldsymbol{h}}_{k,j}} \sum_{l=1}^{i} \alpha^{i-l} \left\| b_k(l) \begin{bmatrix} \mathbf{0}_{d_k} \\ \tilde{\mathcal{C}}_k \\ \mathbf{0}_{M-d_k} \end{bmatrix} \hat{\boldsymbol{h}}_k(i) - \boldsymbol{y}^c_{k,j}(l) \right\|^2 \qquad (19)$$

where b_k is the desired signal provided by a pilot channel and $\boldsymbol{y}_k^c$ the $2M \times 1$ received signal at two consecutive symbol intervals of sensor j and stage k expressed as

$$\boldsymbol{y}^c_{k,j}(i) = \boldsymbol{r}^c_j(i) - \left(\sum_{m=1}^{k-1} \hat{A}_m(i-1)\hat{b}_m(i-1)\begin{bmatrix} \bar{\mathcal{C}}_m \\ \mathbf{0}_M \end{bmatrix}\hat{\boldsymbol{h}}_{m,j}(i-1) \right.$$

$$+ \hat{A}_m(i)\hat{b}_m(i)\begin{bmatrix} \mathbf{0}_{d_m} \\ \tilde{\mathcal{C}}_m \\ \mathbf{0}_{M-d_m} \end{bmatrix}\hat{\boldsymbol{h}}_{m,j}(i)$$

$$\left. + \hat{A}_m(i+1)\hat{b}_m(i+1)\begin{bmatrix} \mathbf{0}_M \\ \mathcal{C}_m \end{bmatrix}\hat{\boldsymbol{h}}_{m,j}(i+1) \right) \qquad (20)$$

The solution to the optimisation problem in (19) is given by

$$\hat{\boldsymbol{h}}_{k,j}(i) = \left(\begin{bmatrix} \mathbf{0}_{d_k} \\ \tilde{\mathcal{C}}_k \\ \mathbf{0}_{M-d_k} \end{bmatrix}^H \begin{bmatrix} \mathbf{0}_{d_k} \\ \tilde{\mathcal{C}}_k \\ \mathbf{0}_{M-d_k} \end{bmatrix} \right)^{-1} \boldsymbol{d}_{k,j}(i) \qquad (21)$$

where

$$\boldsymbol{d}_{k,j}(i) = \sum_{l=1}^{i} \alpha^{i-1} \begin{bmatrix} \mathbf{0}_{d_k} \\ \tilde{\mathcal{C}} \\ \mathbf{0}_{M-d_k} \end{bmatrix}^H \boldsymbol{y}^c_{k,j}(l) b^*_K(l) \qquad (22)$$

The $JL_p \times 1$ space–time channel vector estimate $\hat{\mathcal{H}}_k(i)$ is constructed with the channel estimates of each sensor $\hat{\boldsymbol{h}}_{k,j}(i)$ as described by

$$\hat{\mathcal{H}}_k(i) = [\hat{\boldsymbol{h}}^{\mathrm{T}}_{k,1}(i)\hat{\boldsymbol{h}}^{\mathrm{T}}_{k,2}(i)\dots\hat{\boldsymbol{h}}^{\mathrm{T}}_{k,J}(i)]^{\mathrm{T}} \qquad (23)$$

The $JM \times 1$ spatial signature estimates are then formed according to

$$\hat{\bar{\boldsymbol{p}}}_k^{d_k} = \bar{\mathcal{F}}_k \hat{H}_k(i) \quad \text{and} \quad \hat{\boldsymbol{p}}_k^{d_k} = \mathcal{F}_k \hat{\mathcal{H}}_k(i) \qquad (24)$$

Note that we assume for the channel estimation method that the amplitude is absorbed into the cost function since it is obtained from a similar optimisation problem. This does not affect the performance of the channel estimators as verified in our studies and reported in [10]. In what follows, we address the amplitude estimation task.

4.2.2 Amplitude estimation: The amplitude has to be estimated at the receiver in order to provide this information for different tasks such as IC and power control. Interference cancellers such as SIC need some form of amplitude estimation in order to proceed with the cancellation of the associated users/interferers. This has been reported in [7, 9, 10]. To estimate the amplitudes of the associated user signals, we describe an algorithm that employs the following criterion

$$\hat{A}_{k,j}(i) = \arg\min_{A_{k,j}} E[\|A_{k,j}(i)\hat{b}_k(i)\hat{\tilde{\boldsymbol{p}}}_{k,j}(i) - \boldsymbol{y}^{(k)}(i)\|^2] \quad (25)$$

where the signature at each sensor j is

$$\hat{\tilde{\boldsymbol{p}}}_{k,j}(i) = \begin{bmatrix} \mathbf{0} \\ \tilde{\mathcal{C}}_k \\ \mathbf{0}_{M-d_k} \end{bmatrix} \hat{\boldsymbol{h}}_{k,j}(i)$$

Because the amplitude is identical at each sensor, our studies reveal that it suffices to carry out the estimation procedure for a single sensor. Thus, we describe a stochastic gradient algorithm to estimate the amplitude of user k

$$\hat{A}_k(i+1) = \hat{A}_k(i) - \mu(\hat{A}_k(i)\hat{\tilde{\boldsymbol{p}}}^H_{k,j}(i)\hat{\tilde{\boldsymbol{p}}}_{k,j}(i) - b^*_k(i)\boldsymbol{y}^{(k)H}(i)\hat{\tilde{\boldsymbol{p}}}_{k,j}(i)) \quad (26)$$

5 LS design for the STAR processor

In this section, we describe the parameter estimation procedure for the STAR processor. The exponentially weighted LS design of $\boldsymbol{w}_k$ and $\boldsymbol{v}_k$ considers the cost function given by

$$J_{\text{LS}}^{(\boldsymbol{w}_k,\boldsymbol{v}_k)} = \sum_{l=1}^{i} \alpha^{i-1}|b_k(l) - \boldsymbol{v}_k^H \Re(l)\boldsymbol{w}_k^*|^2 \quad (27)$$

By fixing $\boldsymbol{v}_k$, taking the gradient of (27) with respect to $\boldsymbol{w}_k$ and equating it to a null vector, the interpolated filter/receiver weight vector that minimises (27) is

$$\boldsymbol{w}_k(i) = \gamma(\boldsymbol{v}_k) = \overline{\boldsymbol{R}}_k^{-1}(i)\overline{\boldsymbol{p}}_k(i) \quad (28)$$

where $\bar{\boldsymbol{r}}_k(i) = \Re^{\mathrm{T}}(i)\boldsymbol{v}_k^*(i)$, $\bar{\boldsymbol{p}}_k(i) = \sum_{l=1}^{i} \alpha^{i-1}b_k^*(l)\bar{\boldsymbol{r}}_k(l)$ and $\bar{\boldsymbol{R}}_k(i) = \sum_{l=1}^{i}\alpha^{i-l}\bar{\boldsymbol{r}}_k(l)\bar{\boldsymbol{r}}_k^H(l)$. For SIC receivers, the LS design employs $\bar{\boldsymbol{y}}_k$ instead of $\bar{\boldsymbol{r}}_k$. By fixing $\boldsymbol{w}_k$, taking the gradient of (27) with respect to $\boldsymbol{v}_k$ and equating it to a null vector, the interpolator weight vector that minimises (27) is

$$\boldsymbol{v}_k(i) = \beta(\boldsymbol{w}_k) = \overline{\boldsymbol{R}}_{\boldsymbol{u}_k}^{-1}(i)\overline{\boldsymbol{p}}_{\boldsymbol{u}_k}(i) \quad (29)$$

where $\boldsymbol{u}_k(i) = \Re(i)\boldsymbol{w}_k^*(i)$, $\bar{\boldsymbol{p}}_{\boldsymbol{u}_k}(i) = \sum_{l=1}^{i}\alpha^{i-1}b_k^*(l)\boldsymbol{u}_k(l)$ and $\bar{\boldsymbol{R}}_{\boldsymbol{u}_k}(i) = \sum_{l=1}^{i} \alpha^{i-1}\boldsymbol{u}_k(l)\boldsymbol{u}_k^H(l)$. The associated sum of error squares (SES) expressions are

$$J(\boldsymbol{v}_k) = J_{\text{LS}}(\gamma(\boldsymbol{v}_k), \boldsymbol{v}_k) = \varepsilon_b - \bar{\boldsymbol{p}}_k^H(i)\overline{\boldsymbol{R}}_j^{-1}(i)\overline{\boldsymbol{p}}_k(i) \quad (30)$$

$$J_{\text{LS}}(\boldsymbol{w}_k, \beta(\boldsymbol{w}_k)) = \varepsilon_b - \boldsymbol{p}_{\boldsymbol{u}_k}^H(i)\boldsymbol{R}_{\boldsymbol{u}_k}^{-1}(i)\boldsymbol{p}_{\boldsymbol{u}_k}(i) \quad (31)$$

where $\varepsilon_b = \sum_{l=1}^{i}\alpha^{i-l}|b(l)|^2$ is the energy of the desired response. This structure trades-off a full-rank matrix inversion against the inversion of two matrices with rank JM/L and N_I. Note that (28) and (29) are not closed-form solutions for $\boldsymbol{w}_k$ and $\boldsymbol{v}_k$ since (28) is a function of $\boldsymbol{v}_k$ and (29) depends on $\boldsymbol{w}_k$ and it is necessary to iterate (28) and (29) with an initial guess to obtain a solution. An iterative LS solution can be obtained via adaptive algorithms and a discussion of the convergence properties of the method is given in the appendix.

6 Adaptive RLS algorithms and convergence analysis

Here, we present RLS algorithms [20] that jointly estimate the parameters of the reduced rank and interpolator filters of the proposed STAR processor, depicted in Fig. 1, based on the LS criterion presented in the previous section. We provide a convergence analysis of the proposed RLS algorithms and devise analytical expressions for predicting the MSE achieved by the processor. The complexity of the STAR processor equipped with RLS algorithms is then compared with existing methods.

6.1 RLS algorithms

To avoid the inversion of $\bar{\boldsymbol{R}}_k(i)$ required in (28), we use the matrix inversion lemma (MIL) [20], define $\boldsymbol{P}_k(i) = \bar{\boldsymbol{R}}_k^{-1}(i)$ and the gain vector $\boldsymbol{G}_k(i)$

$$\boldsymbol{G}_k(i) = \frac{\alpha^{-1}\boldsymbol{P}_k(i-1)\bar{\boldsymbol{r}}_k(i)}{1+\alpha^{-1}\bar{\boldsymbol{r}}_k^H(i)\boldsymbol{P}_k(i-1)\bar{\boldsymbol{r}}_k(i)} \quad (32)$$

and thus we can rewrite $\boldsymbol{P}_k(i)$ as

$$\boldsymbol{P}_k(i) = \alpha^{-1}\boldsymbol{P}_k(i-1) - \alpha^{-1}\boldsymbol{G}_k(i)\bar{\boldsymbol{r}}_k^H(i)\boldsymbol{P}_k(i-1) \quad (33)$$

By rearranging (32) we have $\boldsymbol{G}_k(i) = \alpha^{-1}\boldsymbol{P}_k(i-1)\bar{\boldsymbol{r}}_k(i) - \alpha^{-1}\boldsymbol{G}_k(i)\bar{\boldsymbol{z}}_k^H(i)\boldsymbol{P}_k(i-1)\bar{\boldsymbol{r}}_k(i) = \boldsymbol{P}_k(i)\bar{\boldsymbol{r}}_k(i)$. Using (28) and the recursion $\boldsymbol{p}_k(i) = \alpha\boldsymbol{p}_k(i-1) + \bar{\boldsymbol{r}}_k(i)b_k^*(i)$ we obtain

$$\boldsymbol{w}_k(i) = \overline{\boldsymbol{R}}_k^{-1}(i)\hat{\boldsymbol{p}}_k(i) = \alpha\boldsymbol{P}_k(i)\boldsymbol{p}_k(i-1) + \boldsymbol{P}_k(i)\bar{\boldsymbol{r}}_k(i)b_k^*(i) \quad (34)$$

Substituting (33) into (34) yields

$$\boldsymbol{w}_k(i) = \boldsymbol{w}_k(i-1) + \boldsymbol{G}_k(i)\xi_k^*(i) \quad (35)$$

where the a priori estimation error is described by $\xi_k(i) = b_k(i) - \boldsymbol{w}_k^H(i-1)\bar{\boldsymbol{r}}_k(i)$. Similar recursions for the interpolator are devised by using (29). To avoid the inversion of $\bar{\boldsymbol{R}}_{\boldsymbol{u}_k}$ we use the MIL again, define $\boldsymbol{P}_{\boldsymbol{u}_k}(i) = \bar{\boldsymbol{R}}_{\boldsymbol{u}_k}(i)$ and $\boldsymbol{G}_{\boldsymbol{u}_k}(i)$ as

$$\boldsymbol{G}_{\boldsymbol{u}_k}(i) = \frac{\alpha^{-1}\boldsymbol{P}_{\boldsymbol{u}_k}(i-1)\boldsymbol{u}_k(i)}{1+\alpha^{-1}\boldsymbol{u}_k^H(i)\boldsymbol{P}_{\boldsymbol{u}_k}(i-1)\boldsymbol{u}_k(i)} \quad (36)$$

and thus we can rewrite $\boldsymbol{P}_{\boldsymbol{u}_k}(i)$ as

$$\boldsymbol{P}_{\boldsymbol{u}_k}(i) = \alpha^{-1}\boldsymbol{P}_{\boldsymbol{u}_k}(i-1) - \alpha^{-1}\boldsymbol{G}_{\boldsymbol{u}_k}(i)\boldsymbol{u}_k^H(i)\boldsymbol{P}_{\boldsymbol{u}_k}(i-1) \quad (37)$$

By proceeding in a similar approach to obtain (35) we arrive at

$$\boldsymbol{v}_k(i) = \boldsymbol{v}_k(i-1) + \boldsymbol{G}_{V_k}(i)\xi_k^*(i) \quad (38)$$

A summary of the proposed RLS algorithms is given in Table 1.

Table 1: RLS algorithms for the design of proposed STAR processor

Initialise $\boldsymbol{w}_k(0) = [0 \cdots 0]^{\mathrm{T}}$ and $\boldsymbol{v}_k(0) = [1\ 0 \cdots 0]^{\mathrm{T}}$
Choose parameters L, N_I and α
for each time instant (i) do
Compute $JM \times 1$ vector $\boldsymbol{r}_k(i)$ and $N_I \times 1$ vector $\boldsymbol{u}_k(i)$
Obtain $JM/L \times 1$ vector $\bar{\boldsymbol{r}}_k(i) = \boldsymbol{D}\boldsymbol{r}_k(i)$
Compute $JM/L \times JM/L$ matrix $\boldsymbol{P}_k(i)$ and $JM \times 1$ vector $\boldsymbol{G}_k(i)$
Calculate $N_I \times N_I$ matrix $\boldsymbol{P}_{\boldsymbol{u}_k}(i)$ and $N_I \times 1$ vector $\boldsymbol{G}_{\boldsymbol{u}_k}(i)$
Compute $\boldsymbol{v}_k(i) = \boldsymbol{v}_k(i-1) + \boldsymbol{G}_{\boldsymbol{v}_k}(i)\xi_k^*(i)$
Compute $\boldsymbol{w}_k(i) = \boldsymbol{w}_k(i-1) + \boldsymbol{G}_k(i)\xi_k^*(i)$
Reduced-rank estimate: $x_k(i) = \boldsymbol{w}_k^H(i)\bar{\boldsymbol{r}}_k(i)$

6.2 Convergence analysis

This section is devoted to the MSE analysis of the proposed RLS algorithms. Even though this work focuses on asynchronous systems, it is very difficult to analyse these estimators when the input vectors are statistically dependent. For this reason and in order to provide substantial insight with respect to the reduced-rank method and processor, our analysis deals with synchronous DS-CDMA systems [1] ($d_k = 0$ for $k = 1, \ldots, K$) and exploits the so-called Independence Theory [1, 20].

To proceed, let us drop the user k index for ease of presentation and define the tap error vectors $\boldsymbol{e}_w(i)$ and $\boldsymbol{e}_v(i)$ at time index (i)

$$\boldsymbol{e}_w(i) = \boldsymbol{w}(i) - \boldsymbol{w}_{\rm opt}, \quad \boldsymbol{e}_v(i) = \boldsymbol{v}(i) - \boldsymbol{v}_{\rm opt} \tag{39}$$

where $\boldsymbol{w}_{\rm opt}$ and $\boldsymbol{v}_{\rm opt}$ are the optimum tap vectors that achieve the SES for the STAR structure. Because of the unique feature of the joint optimisation of $\boldsymbol{w}(i)$ and $\boldsymbol{v}(i)$, outlined in the appendix, it suffices to study the convergence of only one of the parameters since they will converge to the same solution. By using a similar analysis to [20] and replacing the expected value operator with time averages, let us express the weight-error vector of the reduced-rank solution

$$\boldsymbol{e}_w(i) = \boldsymbol{w}(i) - \boldsymbol{w}_{\rm opt} = \hat{\bar{\boldsymbol{R}}}^{-1}(i) \sum_{l=1}^{i} \boldsymbol{r}(l) e_o^*(l) \tag{40}$$

Using the definition for the weight-error correlation matrix $\boldsymbol{K}(i) = E[\boldsymbol{e}_w(i)\boldsymbol{e}_w^H(i)]$ [20] we have

$$\boldsymbol{K}(i) = E\left[\hat{\bar{\boldsymbol{R}}}^{-1}(i) \sum_{l=1}^{i}\sum_{j=1}^{i} \boldsymbol{r}(l) e_o^*(l) e_o(j) \boldsymbol{r}^H(j) \hat{\bar{\boldsymbol{R}}}^{-1}(i)\right] \tag{41}$$

Assuming that $e_o(i)$ is taken from a zero-mean Gaussian process with variance σ^2, we have

$$E[e_o(l) e_o^*(j)] = \begin{cases} \sigma^2, & l = j \\ 0, & l \neq j \end{cases}$$

and

$$\boldsymbol{K}(i) = \sigma^2 E\left[\hat{\bar{\boldsymbol{R}}}^{-1}(i) \sum_{l=1}^{i}\sum_{j=1}^{i} \boldsymbol{r}(l) \boldsymbol{r}^H(j) \hat{\bar{\boldsymbol{R}}}^{-1}(i)\right] = \sigma^2 E[\hat{\bar{\boldsymbol{R}}}^{-1}(i)] \tag{42}$$

By invoking the independence theory and using the fact that the estimate of the covariance matrix given by $\hat{\bar{\boldsymbol{R}}}^{-1}(i)$ is described by a complex Wishart distribution [20, Section 13.6], the expected value of the time-averaged estimate $\hat{\bar{\boldsymbol{R}}}^{-1}(i)$ is exactly

$$E[\hat{\bar{\boldsymbol{R}}}^{-1}(i)] = \frac{1}{i - JM/L - 1} \bar{\boldsymbol{R}}^{-1}, \quad i > JM/L + 1 \tag{43}$$

where $\bar{\boldsymbol{R}}^{-1}$ is the theoretical reduced-rank covariance matrix and thus

$$\boldsymbol{K}(i) = \frac{\sigma^2 \bar{\boldsymbol{R}}^{-1}}{i - M/L - 1}, \quad i > JM/L + 1 \tag{44}$$

By considering the a priori estimation error $\xi(i)$ as

$$\xi(i) = e_o(i) - \boldsymbol{e}_w^H(i-1)\boldsymbol{r}(i) \tag{45}$$

and expressing its mean-squared value we have

$$\begin{aligned} J'(i) &= E[|\xi(i)|^2] \\ &= E[|e_o(i)|^2] + E[\boldsymbol{r}^H(i)\boldsymbol{e}_w(i-1)\boldsymbol{e}_w^H(i-1)\boldsymbol{r}(i)] \\ &\quad - E[\boldsymbol{e}_w^H(i-1)\boldsymbol{r}(i)e_o^*(i)] - E[e_o(i)\boldsymbol{r}^H(i)\boldsymbol{e}_w(i-1)] \end{aligned} \tag{46}$$

By exploiting the fact that the measurement $e_o(i)$ is zero mean with variance σ^2, the statistical independence between the elements in the third and fourth terms of the above equation, we may simplify the results in (46) and express the MSE of the proposed RLS algorithm as

$$J'(i) = \sigma^2 + {\rm tr}[\bar{\boldsymbol{R}}\boldsymbol{K}(i)] = \sigma^2 + \frac{\sigma^2 JM/L}{i - JM/L - 1}, \quad i > JM/L + 1 \tag{47}$$

The above result shows that the learning curve of the RLS algorithm with the STAR structure converges in about $2JM/L$ iterations, in contrast to the RLS with the full-rank scheme, that requires about $2JM$ iterations. This means that the proposed scheme converges L times faster than the full-rank approach with RLS techniques. Another observation from (47) is that as i increases the excess MSE tends to zero (for $\alpha = 1$) and it is independent from the eigenvalue spread of the matrix $\hat{\bar{\boldsymbol{R}}}^{-1}(i)$.

6.3 Computational complexity: Here, we illustrate the computational complexity of the proposed structure and algorithms and compare it with existing RLS algorithms, as shown in Table 2. The STAR processor trades-off a computational complexity of $O((JM)^2)$ required by the full-rank RLS against two RLS algorithms operating in parallel, with complexity $O((JM/L)^2)$ and $O(N_I^2)$. If the designer chooses a small N_I and the decimation factor $L \geq 2$ then the complexity can be greatly reduced. Note that the MWF technique has a complexity $O(D\overline{JM}^2)$, where the variable dimension of the vectors $\overline{JM} = JM - d$ varies according to the orthogonal decomposition and the rank $d = 1, \ldots, D$.

In Fig. 3, we depict the curves that describe the computational complexity in terms of the arithmetic operations (additions and multiplications) as a function of the number of parameters JM for $L_{\rm p} = 9$ and $D = 4$. The curves indicate a significant computational advantage of the STAR over the full-rank design. In comparison with the existing MWF reduced-rank technique, the proposed STAR processor is also substantially less complex and more flexible in all situations since the designer can choose the decimation factor L, allowing variable complexity requirements.

Table 2: Computational complexity of RLS adaptation algorithms

Algorithm	Number of operations per symbol: Additions	Multiplications
Full-rank	$3(JM-1)^2$ $+(JM)^2+2JM$	$6(JM)^2$ $+2JM+2$
STAR	$3(\frac{JM}{L}-1)^2 + 3(N_I-1)^2$ $+(\frac{JM}{L}-1)N_I$ $+N_IJM+(\frac{JM}{L})^2$ $+N_I^2+2\frac{JM}{L}+2N_I$	$6(\frac{JM}{L})^2+6N_I^2$ $+\frac{JM}{L}N_I$ $+3\frac{JM}{L}$ $+N_I+2$
MWF	$D(4(\overline{JM}-1)^2+2\overline{JM})$	$D(4\overline{JM}^2+2\overline{JM}+3)$

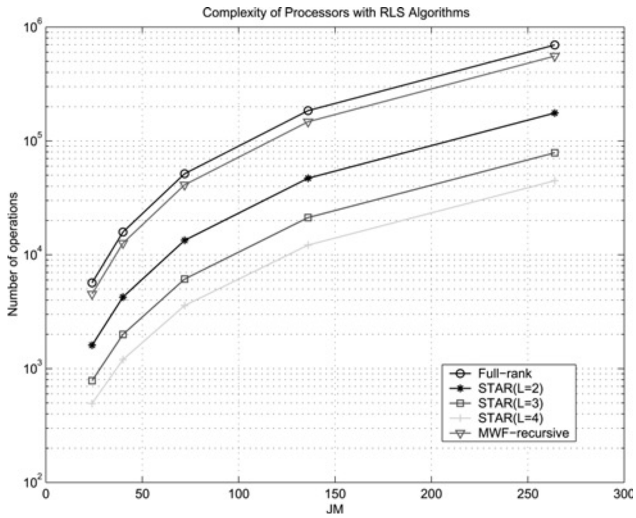

Fig. 3 *Complexity in terms of arithmetic operation against the number of received samples (JM) for analysed processors*

7 Simulations

In this section, we evaluate the analytical results developed in Section 6.2 for the STAR processor and RLS algorithms. We also assess the bit-error rate (BER) performance of the STAR system with $J = 1$ and 3 antenna elements and compare it with the full-rank [3] (without and with known channels and DoAs) and the MWF [16] with antenna-array schemes using the proposed linear and SIC detectors. The full-rank receiver with known channels and DoAs corresponds to the minimum MSE receiver with the filter constructed with the effective signature sequences and the noise variance. Note that the work in [17] considers different versions of the original MWF [14] with detectors incorporating diversity, while here we consider the space–time MWF scheme of [16] and extend it to a SIC structure. In our comparisons, it should be remarked that we selected computational efficient versions of the MWF which are equivalent to RLS algorithms, as reported in [15]. Thus the comparison involves algorithms of the same type for fairness.

The DS-CDMA system employs Gold sequences of length $N = 31$ and all channels assume that $L_p = 9$ as an upper bound. Another important issue in our studies is the interpolator filter $\boldsymbol{v}_k$ design. We have conducted experiments in order to obtain the most adequate dimension for $\boldsymbol{v}_k(i)$, with values ranging from $N_I = 3$ to 6 (note that for $N_I < 3$ the new scheme did not perform well and using $N_I < 6$ was unnecessary). The results for a wide range of scenarios indicate that performance is not sensitive to an increase in the number of taps in $\boldsymbol{v}_k(i)$. This is because the reduced-rank projection based on the combined use of an adaptive interpolator and an adaptive reduced-rank filter is not able to compensate for the decimation with only 1 or 2 elements in the interpolator. When the interpolator size becomes reasonably large (greater than 6), there is no improved modelling and the adaptation becomes slower in the proposed subspace projection. Thus, for this reason and to keep the complexity low, we selected $N_I = 3$ for the remaining experiments.

7.1 MSE convergence performance: analytical results

Here, we verify that the results (47) given in Section 6.2 on convergence analysis of the STAR processor can provide a means of estimating its MSE performance. The steady-state MSE between the desired and the estimated symbol by the space–time processor with linear receivers obtained through simulation is compared with those computed with the expressions derived in Section 6.2. To illustrate the usefulness of our analysis, we carried out experiments, where the channels have three paths with random complex gains, are normalised to unit power, the system is made synchronous ($d_k = 0$ for $k = 1, \ldots, K$), the DoAs are uniformly distributed in a sector with 120°, the RLS algorithms use $\alpha = 1$ and the spacing between paths is obtained from a discrete uniform random variable between 1 and 3 chips for each run in a scenario with perfect power control. The experiments are averaged over 1000 independent runs and over the user population.

The results, shown in Fig. 4 for $J = 1$ and 3, indicate that the analytical results closely match those obtained through simulation upon convergence, confirming the validity of our analysis. Specifically, we verify that the use of antenna arrays ($J = 3$) can significantly improve the MSE performance as compared with the single-antenna version through the use of spatial filtering and the improved rejection of interferers. Also, the adaptive reduced-rank estimators converge in about $2M/L$ symbols, which agrees with the theory detailed in Section 6.2.

7.2 BER performance

In this section, we show the average BER performance of the proposed space–time adaptive linear and SIC multiuser receivers. The parameters of the algorithms are optimised (number of stages $D = 4$ of MWF, interpolator length $N_I = 3$ and $\alpha = 0.998$ for RLS algorithms [20]). The channels experienced by different users are i.i.d. whose coefficients for each user k are $h_{k,m}(i) = p_{k,m}\lambda_{k,m}(i)$, where $\lambda_{k,m}(i)$ ($m = 0, 1, \ldots, L_p - 1$, $E[|\lambda_{k,m}(i)|^2] = 1$) are obtained with Clarke's model [21]. The results are shown in terms of the normalised Doppler frequency $f_d T$ (cycles/symbol) and we use three-path channels with relative powers $p_{k,m}^2$ given by 0, −3 and −6 dB, where in each run the spacing between paths is obtained from a discrete uniform random variable between 1 and 3 chips. The

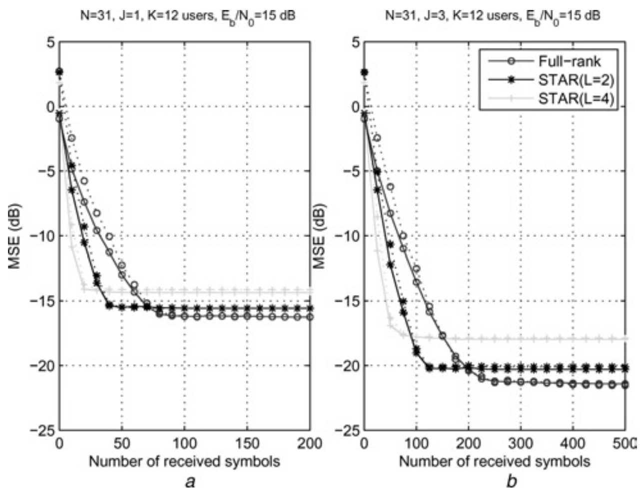

Fig. 4 *MSE for analytical and simulated results against the number of received symbols for processors with linear receivers using*

a $J = 1$
b $J = 3$
Solid lines stand for simulated results, whereas dotted lines correspond to analytical results

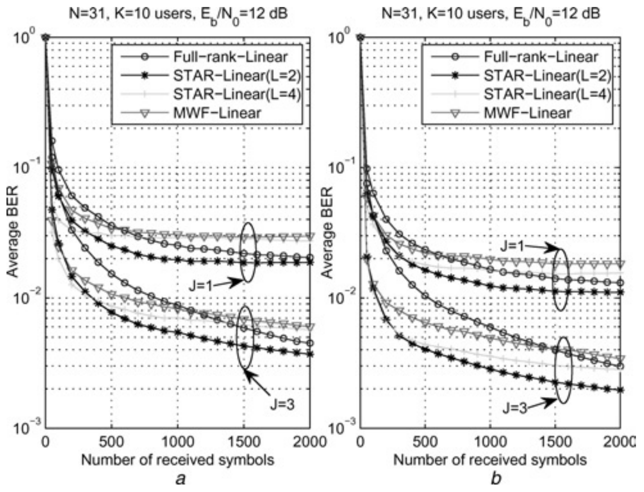

Fig. 5 *Average BER performance against the number of received symbols with $f_d T = 0.0005$ for*

a Linear
b SIC receivers

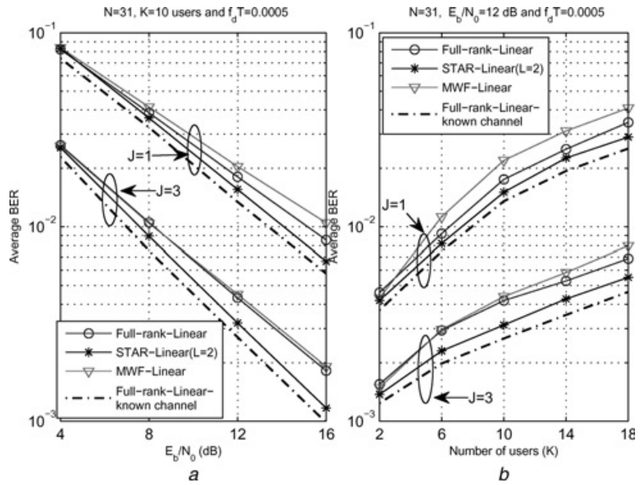

Fig. 7 *BER performance against*

a E_b/N_0
b Number of users

unknown DOAs $\phi_{k,m}$ for each path and user are uniformly distributed between 0 and $2\pi/3$ (120°) for all simulations and the delay d_k of the users that describe the system asynchronism is taken from a discrete uniform random variable between 0 and 30 chips. The system has a power distribution among the users for each run that follows a log-normal distribution with associated standard deviation of 3 dB and all experiments are averaged over 1000 trials and over the users in the system.

To assess the BER convergence performance of the space–time processors against time, the adaptive linear and SIC receivers are adjusted with 200 symbols during the training period and then switch to decision-directed mode for the remaining 1800 symbols. The results, illustrated in Fig. 5, show that the reduced-rank methods significantly outperform the full-rank receiver and the best performance is obtained by the proposed STAR processor. For small data support, the STAR with $L = 4$ can achieve improved performance over the STAR with $L = 2$. However, as the data support is increased, the STAR with $L = 2$ is able to outperform the processor with $L = 4$ at steady state. This is because the reduced-rank scheme trades-off a faster convergence performance against a higher MSE or BER performance at steady state. With a higher decimation factor (e.g. $L = 4$ against $L = 2$), the proposed scheme is able to converge faster but loses degrees of freedom to achieve a lower BER at steady state. The proposed SIC receivers outperform the linear schemes and as the number of antenna elements J is increased so is the performance. In particular, the convergence speed of receivers is further increased through the use of reduced-rank techniques combined with IC carried out by the proposed SIC detectors. The STAR offers extra flexibility since the designer can adjust L in order to trade-off faster response against improved steady-state performance.

We also consider the average BER performance of adaptive linear and SIC receivers against E_b/N_0 and number of users, as depicted in Figs. 6 and 7, respectively. The receivers are adjusted with 200 symbols during the training period, then switch to decision directed mode and process 2000 data symbols. The curves are averaged over 1000 independent trials and over the K users.

The results show that the proposed STAR processor with $L = 2$ achieves the best BER performance, followed by the full-rank and the MWF. Specifically, the STAR with $L = 2$ can save up to 1 dB in E_b/N_0 as compared with full-rank estimator for the same BER performance. The STAR processors are capable of approaching the performance of the full-rank scheme with perfect channel knowledge at much lower complexity. In terms of system capacity, the gains are more pronounced for the receivers equipped with more sensors in the antenna array and a comparison between the results for linear and SIC receivers (Figs. 6 and 7) shows that SIC receivers are considerably better than linear ones. Specifically, the plots show that the SIC receivers accommodate up to 4 more users than the linear detectors with $J = 1$, whereas the space–time SIC schemes handle up to 6 more users than the linear ones with $J = 3$, for the same BER performance.

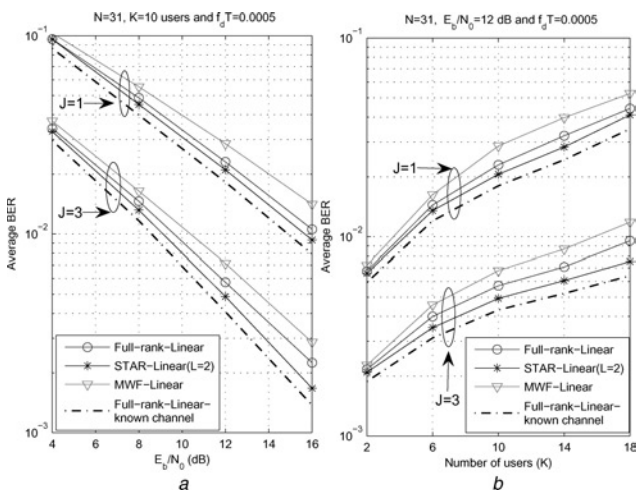

Fig. 6 *BER performance against*

a E_b/N_0
b Number of users

8 Conclusions

A flexible STAR processor for interference suppression in DS-CDMA systems with RLS algorithms was proposed. Linear and SIC space–time receivers with antenna arrays based on reduced-rank STAR processors were introduced and investigated in an uplink scenario. The results have shown that the STAR reduced-rank processors can achieve superior performance to full-rank and the MWF reduced-rank schemes and that the proposed SIC receiver is significantly better than the linear detector.

9 Acknowledgment

This work was supported in part by the Brazilian Council for Scientific and Technological Development (CNPq).

10 References

1 Honig, M.L., and Poor, H.V.: 'Adaptive interference suppression' in Poor, H.V., and Wornell, G.W. (Eds.): 'Wireless Communications: Signal Processing Perspectives' (Prentice-Hall, Englewood Cliffs, NJ, 1998), ch. 2, pp. 64–128
2 Verdu, S.: 'Multiuser detection' (Cambridge, 1998)
3 Paulraj, A., Nabar, R., and Gore, D.: 'Introduction to space–time wireless communications' (Cambridge, 2003)
4 Yener, A., Yates, R.D., and Ulukus, S.: 'Combined multiuser detection and beamforming for CDMA systems: filter structures', *IEEE Trans, Veh. Technol.*, 2002, **51**, (5), pp. 1087–1095
5 Lupas, R., and Verdu, S.: 'Linear multiuser detectors for synchronous code-division multiple-access channels', *IEEE Trans. Inf. Theory*, 1989, **35**, pp. 123–136
6 Abdulrahman, M., Sheikh, A.U.K., and Falconer, D.D.: 'Decision feedback equalization for CDMA in indoor wireless communications', *IEEE J. Sel. Areas Commun.*, 1994, **12**, (4), pp. 698–706
7 Patel, P., and Holtzman, J.: 'Analysis of a simple successive interference cancellation scheme in a DS/CDMA systems', *IEEE J. Sel. Areas Commun.*, 1994, **12**, (5), pp. 796–807
8 Varanasi, M.K., and Aazhang, B.: 'Multistage detection in asynchronous CDMA communications', *IEEE Trans. Commun.*, 1990, **38**, (4), pp. 509–519
9 Cho, Y., and Lee, J.H.: 'Analysis of an adaptive SIC for near–far resistant DS-CDMA', *IEEE Trans. Commun.*, 1998, **46**, (11), pp. 1429–1432
10 Lai, K.C., and Shynk, J.J.: 'Steady-state analysis of the adaptive successive interference canceler for DS/CDMA signals', *IEEE Trans. Signal Process.*, 2001, **49**, (10), pp. 2345–2362
11 Haimovich, A.M., and Bar-Ness, Y.: 'An eigenanalysis interference canceler', *IEEE Trans. Signal Process*, 1991, **39**, pp. 76–84
12 Wang, X., and Poor, H.V.: 'Blind multiuser detection: a subspace approach', *IEEE Trans. Inf. Theory*, 1998, **44**, pp. 677–690
13 Song, Y., and Roy, S.: 'Blind adaptive reduced-rank detection for DS-CDMA signals in multipath channels', *IEEE J. Sel. Areas Commun.*, 1999, **17**, pp. 1960–1970
14 Goldstein, J.S., Reed, I.S., and Scharf, L.L.: 'A multistage representation of the Wiener filter based on orthogonal projections', *IEEE Trans. Inf. Theory*, 1998, **44**, pp. 2943–2959
15 Honig, M.L., and Goldstein, J.S.: 'Adaptive reduced-rank interference suppression based on the multistage Wiener filter', *IEEE Trans. Commun.*, 2002, **50**, (6), pp. 986–994
16 Hu, C.C., and Reed, I.S.: 'Space–time adaptive reduced-rank multistage Wiener filtering for asynchronous DS-CDMA', *IEEE Trans. Signal Process.*, 2004, **52**, (7), pp. 1862–1877
17 Wu, S.-H., Mitra, U., and Kuo, C.-C.J.: 'Reduced-rank multistage receivers for DS-CDMA in frequency-selective fading channels', *IEEE Trans. Commun.*, 2005, **53**, (2), pp. 2609–2614
18 de Lamare, R.C., and Sampaio-Neto, R.: 'Adaptive reduced-rank MMSE filtering with interpolated FIR filters and adaptive interpolators', *IEEE Signal Process. Lett.*, 2005, **12**, (3), pp. 177–180
19 Baissas, M.-A.R., and Sayeed, A.M.: 'Pilot-based estimation of time varying multipath channels for coherent CDMA receivers', *IEEE Trans. Signal Process.*, 2002, **50**, (8), pp. 2037–2049
20 Haykin, S.: 'Adaptive filter theory' (Prentice-Hall, Englewood Cliffs, NJ, 2002, 4th edn.)
21 Rappaport, T.S.: 'Wireless communications' (Prentice-Hall, Englewood Cliffs, NJ, 1996)
22 Bertsekas, D.P.: 'Nonlinear programming' (Athena Scientific, 1999, 2nd edn.)

11 Appendix: convergence properties

The importance of this investigation lies on the establishment that the design of the proposed STAR processor is based on joint optimisation problem that has a unique solution and does not present local minima. To study the convergence properties of the interpolated LS design, we consider the associated SES expressions in (30) and (31). We note that points of global minimum of $J_{\rm LS}(\boldsymbol{w}_k, \boldsymbol{v}_k) = \sum_{l=1}^{i} \alpha^{i-l} |b_k(l) - \boldsymbol{v}_k^H \Re(l) \boldsymbol{w}_k^*|^2$ can be obtained by $\boldsymbol{v}_{\rm opt} = \arg\min_{\boldsymbol{v}_k} J(\boldsymbol{v}_k)$ and $\boldsymbol{w}_{\rm opt} = \gamma(\boldsymbol{v}_{\rm opt})$ or $\boldsymbol{w}_{\rm opt} = \arg\min_{\boldsymbol{w}_k} J_{\rm LS}(\beta(\boldsymbol{w}_k), \boldsymbol{w}_k)$ and $\boldsymbol{v}_{\rm opt} = \beta(\boldsymbol{w}_{\rm opt})$. At a minimum point $J_{\rm LS}(\boldsymbol{v}_k, \gamma(\boldsymbol{v}_k))$ equals $J_{\rm LS}(\beta(\boldsymbol{w}_k), \boldsymbol{w}_k)$ and the minimum SES for the proposed structure is achieved. We further note that since $J(\boldsymbol{v}_k) = J(t\boldsymbol{v}_k)$, for every $t \neq 0$, then if $\boldsymbol{v}_k^{\star}$ is a point of global minimum of $J(\boldsymbol{v}_k)$ then $t\boldsymbol{v}_k^{\star}$ is also a point of global minimum. Therefore points of global minimum (optimum interpolator filters) can be obtained by $\boldsymbol{v}_k^{\star} = \arg\min_{\|\boldsymbol{v}_k\|=1} J(\boldsymbol{v}_k)$. Since the existence of at least one point of global minimum of $J(\boldsymbol{v}_k)$ for $\|\boldsymbol{v}_k\| = 1$ is guaranteed by the theorem of Weierstrass [22], then the existence of (infinite) points of global minimum is also guaranteed for the cost function in (27). This establishes the existence of the solution of the optimisation problem. Because at a minimum point (30) equals (31), the designer can consider only one of the parameter vectors, either $\boldsymbol{w}_k$ or $\boldsymbol{v}_k$, for analysis purposes.

In the context of global convergence, a sufficient but not necessary condition is the convexity of the cost function, which is verified if its Hessian matrix is positive semi-definite, that is $\boldsymbol{a}^H \boldsymbol{H} \boldsymbol{a} \geq 0$, for any vector $\boldsymbol{a}$. First, let us consider the minimisation of (27) with fixed interpolators. Such optimisation leads to the following Hessian

$$\boldsymbol{H} = \frac{\partial}{\partial \boldsymbol{w}_k^H} \frac{(J_{\rm LS}(\cdot))}{\partial \boldsymbol{w}_k} = \sum_{l=1}^{i} \alpha^{i-l} \boldsymbol{r}_k(l) \boldsymbol{r}_k^H(l) = \boldsymbol{R}_k(i) \tag{48}$$

which is positive semi-definite and ensures the convexity of the cost function for the case of fixed interpolators. Consider now the joint optimisation of the interpolator $\boldsymbol{v}_k$ and receiver $\boldsymbol{w}_k$ through an equivalent cost function to (27)

$$\tilde{J}_{\rm LS}(\boldsymbol{z}_k) = \sum_{l=1}^{i} \alpha^{i-1} |b(l) - \boldsymbol{z}_k^H \boldsymbol{B}(l) \boldsymbol{z}_k|^2] \tag{49}$$

where

$$\boldsymbol{B}(l) = \begin{bmatrix} \boldsymbol{0} & \boldsymbol{0} \\ \Re(l) & \boldsymbol{0} \end{bmatrix}$$

is an $(N_I + JM/L) \times (N_I + JM/L)$ matrix. The Hessian ($\boldsymbol{H}$) with respect to $\boldsymbol{z}_k = [\boldsymbol{w}_k^{\rm T} \boldsymbol{v}_k^{\rm T}]^{\rm T}$ is

$$\begin{aligned} \boldsymbol{H} = \frac{\partial}{\partial \boldsymbol{z}_k^H} \frac{\partial(\tilde{J}_{\rm LS}(\cdot))}{\partial \boldsymbol{z}_k} &= \left(\sum_{l=1}^{i} \alpha^{i-l} (\boldsymbol{z}_k^H \boldsymbol{B}(l) \boldsymbol{z}_k - b_k(l)) \boldsymbol{B}^H(l) \right) \\ &+ \left(\sum_{l=1}^{i} \alpha^{i-l} (\boldsymbol{z}_k^H \boldsymbol{B}^H(l) \boldsymbol{z}_k - b_k^*(l)) \boldsymbol{B}(l) \right) \\ &+ \left(\sum_{l=1}^{i} \alpha^{i-l} \boldsymbol{B}(l) \boldsymbol{z}_k \boldsymbol{z}_k^H \boldsymbol{B}^H(l) \right) \\ &+ \left(\sum_{l=1}^{i} \alpha^{i-l} \boldsymbol{B}^H(l) \boldsymbol{z}_k \boldsymbol{z}_k^H \boldsymbol{B}(l) \right) \end{aligned} \tag{50}$$

By examining $\boldsymbol{H}$ we note that the third and fourth terms yield positive semi-definite matrices $\boldsymbol{a}^H(\sum_{l=1}^{i} \alpha^{i-l} \boldsymbol{B}(l) \boldsymbol{z}_k \boldsymbol{z}_k^H B^H(l))\boldsymbol{a} \geq 0$ and $\boldsymbol{a}^H(\sum_{l=1}^{i} \alpha^{i-l} \boldsymbol{B}^H(l)\ \boldsymbol{z}_k \boldsymbol{z}_k^H \boldsymbol{B}(l)]\boldsymbol{a}) \geq 0$, $\boldsymbol{z}_k \neq 0$), whereas the first and second terms are indefinite matrices. Thus, the cost function cannot be classified as convex. However, for a gradient search algorithm, a desirable property of the cost function is that it shows no points of local minimum, that is, every point of minimum is a point of global minimum (convexity is a sufficient,

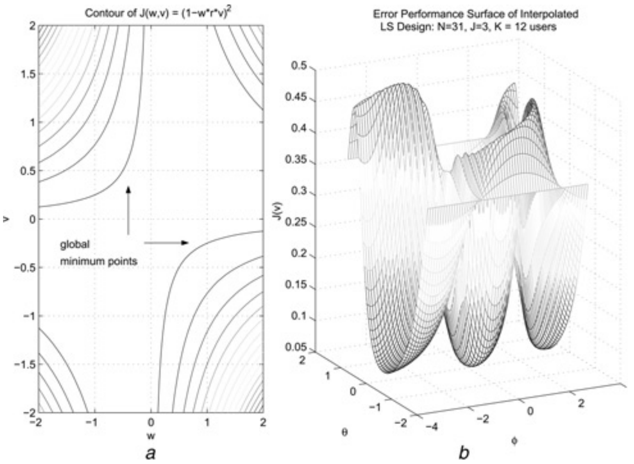

Fig. 8 *Every point of minimum is a point of global minimum*

a Contour plots of the function $f(v, w) = (1 - w * r * v)^2$
b Error-performance surface of space–time interpolated LS receivers at $E_b/N_0 = 15$ dB for $L = 4$

but not necessary, condition for this property to hold) and it is conjectured that the problem in (27) has this property.

To support this claim, we carried out the following studies. First, we considered the scalar case of the function in (27), defined as $f(w,\ v) = (b - wrv)^2 = b^2 - 2b\,wrv + (w\Re v)^2$, where r is a constant. By choosing v (the 'scalar' interpolator) fixed, it is evident that the function $f(w,\ v) = (b - wc)^2$, where c is a constant, is a convex one, whereas for a time-varying interpolator the curves shown in Fig. 8*a*, indicate that the function is no longer convex but it does not exhibit local minima. Secondly, by taking into account that for small interpolator filter length $N_I (N_I > 3)$, $\boldsymbol{v}_k$ can be expressed in spherical coordinates and a surface can be constructed. Specifically, we expressed the parameter vector $\boldsymbol{v}_k$ as

$$\boldsymbol{v}_k = r[\cos(\theta)\cos(\phi)\cos(\theta)\sin(\phi)\sin(\theta)]^{\mathrm{T}}$$

where r is the radius, θ and ϕ were varied from $-\pi/2$ to $\pi/2$ and $-\pi$ to π, respectively, and (27) was plotted for various scenarios. The plot of the error-performance surface of $J(\boldsymbol{v}_k)$, depicted in Fig. 8*b*, reveals that $J(\boldsymbol{v}_k)$ has a global minimum value (as it should) but do not exhibit local minima, which implies that (29) has no local minima either. If the cost function in (27) had a point of local minimum then $J(\boldsymbol{v}_k)$ in (27) should also exhibit a point of local minimum even though the reciprocal is not necessarily true: a point of local minimum of $J(\boldsymbol{v}_k)$ may correspond to a saddle point of $J_{\mathrm{LS}}(\boldsymbol{v}_k, \boldsymbol{w}_k)$, if it exists. In addition, an important feature that advocates the non-existence of local minima is that the algorithm always converge to the same minimum value, for a given experiment, independently of any interpolator initialisation (except for $\boldsymbol{v}_k(0) = [0 \cdots 0]^{\mathrm{T}}$ that eliminates the signal) for several scenarios.